

# Precision Timing Detectors with Cadmium-Telluride Sensor

A. Bornheim<sup>a</sup>, C. Pena<sup>a</sup>, M. Spiropulu<sup>a</sup>, S. Xie<sup>\*,a</sup>, Z. Zhang<sup>a</sup>

<sup>a</sup>*California Institute of Technology, Pasadena, CA, USA*

---

## Abstract

Precision timing detectors for high energy physics experiments with temporal resolutions of a few 10 ps are of pivotal importance to master the challenges posed by the highest energy particle accelerators such as the LHC. Calorimetric timing measurements have been a focus of recent research, enabled by exploiting the temporal coherence of electromagnetic showers. Scintillating crystals with high light yield as well as silicon sensors are viable sensitive materials for sampling calorimeters. Silicon sensors have very high efficiency for charged particles. However, their sensitivity to photons, which comprise a large fraction of the electromagnetic shower, is limited. To enhance the efficiency of detecting photons, materials with higher atomic numbers than silicon are preferable. In this paper we present test beam measurements with a Cadmium-Telluride (CdTe) sensor as the active element of a secondary emission calorimeter with focus on the timing performance of the detector. A Schottky type CdTe sensor with an active area of 1 cm<sup>2</sup> and a thickness of 1 mm is used in an arrangement with tungsten and lead absorbers. Measurements are performed with electron beams in the energy range from 2 GeV to 200 GeV. A timing resolution of 20 ps is achieved under the best conditions.

*Key words:* Cadmium Telluride, Timing, Calorimeter

---

## 1. Introduction

There has been much recent interest in enhancing the timing capability of large particle physics collider experiments to the level of 20 – 30 ps for each final state particle reconstructed in the detector. In order to probe increasingly rare high energy particle interactions, future hadron colliders must provide large instantaneous luminosity well above 10<sup>35</sup> cm<sup>-2</sup>s<sup>-1</sup>. With current accelerator and particle detector capabilities, such a high instantaneous luminosity will result in very large amounts of simultaneous particle collisions, referred to as pileup. For the high luminosity upgrade of the Large Hadron Collider (HL-LHC), pileup is expected to exceed 200 inelastic proton-proton collisions per bunch crossing, when two ensembles of up to 10<sup>12</sup> particles collide at the center of the detectors. In the LHC, the collisions from each bunch crossing are spread out over a length of about 10 cm along the beam axis direction and have an additional time dispersion of about 150 ps. Under such conditions, the task to associate particles measured

---

\*Corresponding author

Email address: [sixie@hep.caltech.edu](mailto:sixie@hep.caltech.edu) (S. Xie)

Preprint submitted to Nucl. Instrum. Meth. A

April 4, 2017

in the detectors to a particular proton collision within a bunch crossing becomes very challenging. Precision timing detectors can be used to recover the ability to discriminate between particles produced by different inelastic collisions [1]. For particle beams with bunch profiles similar to that of the LHC, a detector capable of measuring the time of arrival of a particle with a precision of 20 – 30 ps could reduce the impact of pileup by a factor of 5 to 10.

Highly granular calorimeters based on silicon sensors as the active material have been the focus of recent interest [2, 3], due to radiation hardness considerations as well as maturity of the silicon sensor technology. In this article, we present results of studies of a similar sampling calorimeter prototype using Cadmium-Telluride (CdTe) sensors as the active material. CdTe has been studied extensively in the context of thin film solar cells and has become a mature and wide-spread technology [4]. It is also widely used as a radiation detector for nuclear spectroscopy, and as a sensor for photons in the X-ray range due to its high quantum efficiency in this part of the spectrum [5–8]. This feature is of particular interest in the context of its use in calorimetry because it would enhance the sensitivity to secondary particles in the keV range, a significant component of the electromagnetic shower. Conventional prototypes using silicon sensors have limited sensitivity to photons in this energy range. CdTe sensors are available with thicknesses of several mm which can further enhance the efficiency for X-ray photons as well as the ionization signal yield from charged particles. Therefore, the first study of electromagnetic showers using CdTe sensors has the potential to yield new insight into the behavior of secondary particles produced within an electromagnetic shower with energies in the keV range, and has the potential to yield an improvement on the energy measurement due to the additional contribution of the higher energy X-ray photons to which calorimeters based on silicon sensors are less sensitive to.

The recent interest on precision timing has resulted in new studies of the timing properties of silicon sensors. These studies have found a time resolution at the 20 ps level, provided a sufficiently large signal size in a variety of applications ranging from calorimetry [9] to charged particle detectors [10]. The signal formation process in CdTe sensors is very similar to the process in silicon and has similar potential to yield precise time-stamps.

In this article, we study the signal response of a CdTe sensor to electromagnetic showers of varying energies and at different shower depths. We also study the timing performance of a CdTe sensor for electromagnetic showers.

## 2. CdTe Sensor

The semi-conducting properties of CdTe have been studied for many decades [4], particularly in the the context of photo-voltaic applications. CdTe sensors are also widely used in X-ray detectors [5, 7, 8]. They have also been investigated for synchrotron radiation detectors in accelerator technology [11], and for three dimensional tracking for neutrino-less double-beta decay [12]. In reference [11, 13], poly-crystalline CdTe sensors have been demonstrated to have no significant degradation in performance after irradiation of  $10^{16}$  neutrons/cm<sup>2</sup>. In our previous studies [9, 14–19] we have demonstrated that increasing the primary sensor signal is crucial to achieve good timing resolutions. CdTe sensors are available with thicknesses of 1 mm and more, and the path-length of the charged shower particles in the sensor material scales up accordingly. The higher density

of CdTe compared to Si also increases the energy loss of charged particles. A minimal ionizing particle will create about 50000 electrons in 300  $\mu\text{m}$  of CdTe, compared to 30000 electrons for a Si sensor [13]. The combination of these two effects results in a larger primary signal. Furthermore, CdTe features a significantly higher efficiency for detecting photons in the 10–100 keV energy range compared to silicon sensors. The higher atomic number of Cadmium and Tellurium, averaging to 48.52 for the compound bulk material, results in a higher interaction cross section for photons in this energy range. Secondary photons are abundant in electromagnetic showers. Reference [20] shows that for shower secondaries with energy over 1 MeV, there are 6 to 7 times more photons than electrons. Therefore, an additional increase to the signal size resulting from the secondary photons is a promising possibility. The exact quantitative impact of the secondary photons will further depend on the depth location at which the shower is sampled and the exact material distribution in the vicinity of the sensor.

Our measurements were conducted with a CdTe Schottky type diode purchased from Acrorad [21]. It is 1  $\text{cm}^2$  in transverse size and 1 mm thick. It was operated at a bias voltage of 700 V and the dark current was between 3 nA and 6 nA depending on the environmental conditions in the test-beam experimental zones. The sensor was placed in a box made of 0.3 mm thick copper sheets and located about 3 mm away from the front face of the copper box. A photograph of the sensor and the copper box enclosing it is shown in Figure 1.



Figure 1: Left: CdTe sensor used for the measurements. The sensor is a Schottky type diode with a transverse size of 1  $\text{cm}^2$  and a thickness of 1 mm. The base-plate is biased at 700 V. On the front-left corner of the sensor, the wire bond connection to the metalized top layer of the sensor can be seen. On the back-right corner, the wire bond connection to the base-plate can be seen. Right: A photograph of the copper box enclosing the CdTe sensor.

The electrical circuit shown in Figure 2 was used to connect to the sensor to the bias voltage with a standard high voltage cable and the readout electronics using a SMA cable with a feed through penetrating the copper box.

### 3. Test-beam Setup and Experimental Apparatus

We performed the measurements at the T9 beam-line of the CERN East-Area test-beam facility and the H2 beam-line of the CERN North-Area test-beam facility. The T9 beam-line provides secondary beams of energies ranging between 0.5 GeV and 10 GeV based on the primary proton beam source from the Proton Synchrotron (PS), while the

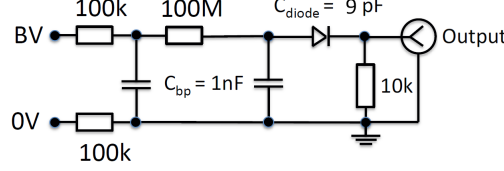


Figure 2: Schematic diagram of the circuit used to polarize and read out the CdTe sensor. The circuit and the sensor are enclosed inside a copper box.

H2 beam-line provides secondary beams of energies ranging between 20 GeV and 400 GeV based on the primary proton beam source from the Super Proton Synchrotron (SPS). The beams are composed of a mixture of electrons and pions. The electron fraction in the beam at H2 is typically larger than 75% while at T9 it is typically about 10%.

Trigger counters made of photo-multipliers coupled to 4 cm × 4 cm plastic scintillators are used to initiate the read out of the data acquisition (DAQ) system. The DAQ system uses a CAEN V1742 switched capacitor digitizer based on the DRS4 chip [22]. Wire chambers are used to measure the position of each incident beam particle in the plane transverse to the beam-line. A stack of lead or tungsten absorbers of different thicknesses are placed about 5 mm in front of the CdTe sensor, which is enclosed within a copper box. The signals from the CdTe sensor are amplified using a Hamamatsu C5594 amplifier [23] with a bandwidth of 1.5 GHz and providing a voltage gain of 36 dB. A 10 dB attenuator was used to attenuate the input signal to the amplifier for beam energies of 50 GeV and above to adjust the CdTe signal to the dynamic range of the amplifier. A micro-channel plate photo-multiplier (MCP-PMT) detector is used to provide a very precise reference time-stamp. At the T9 beam-line, a Hamamatsu R3809U MCP-PMT [24] is placed just upstream of the absorber material. At the H2 beam-line a Photek 240 MCP-PMT [25] is used, which contains a significant amount of absorber material (about 1.8 radiation lengths), and is therefore placed just downstream of the CdTe sensor to avoid inducing an early electromagnetic shower. The precision of the time measurement for both types of MCP-PMTs is less than 10 ps [14, 15]. As the purity of the electron beam at the T9 beam-line is significantly lower than at the H2 beam-line, we use a LYSO crystal optically coupled to an MCP-PMT as a means of discriminating the electrons from the pions in the beam. The LYSO cube is about 1.7cm thick, corresponding to 1.5 radiation lengths, and is placed close to the shower maximum. Therefore, electron particles will produce electromagnetic shower particles which create scintillation light in the LYSO crystal, while pions typically do not. The efficiency for identifying electrons with this method was cross checked using a Cherenkov counter and was observed to be greater than 95%. The entire setup of absorber, reference counter and CdTe sensor box is housed in an aluminum box to provide further shielding against environmental noise. The schematic diagrams of the experimental setups at H2 and T9 are shown in Figure 3, and a photograph of the contents of the aluminum box for the setup at T9 is shown in Figure 4.

The horizontal and vertical position measurements from the wire chamber are used to determine the location of the CdTe sensor relative to the beam and to align the beam. In Figure 5, we show the average amplitude measured in the CdTe sensor after 6 radiation lengths of tungsten absorber as a function of the horizontal and vertical positions as

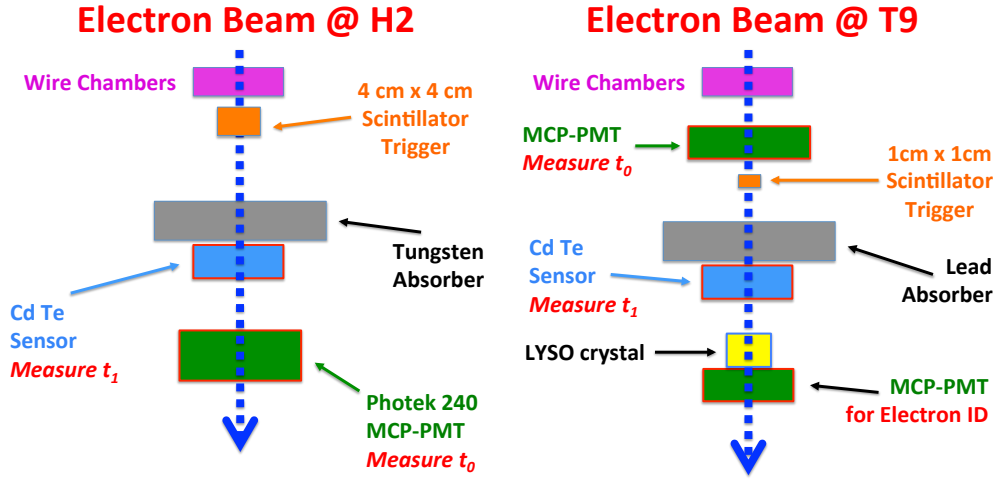


Figure 3: Schematic diagrams of the test-beam setups at H2 (left) and T9 (right) are shown. The time-stamps  $t_0$  and  $t_1$  are defined in Section 4.

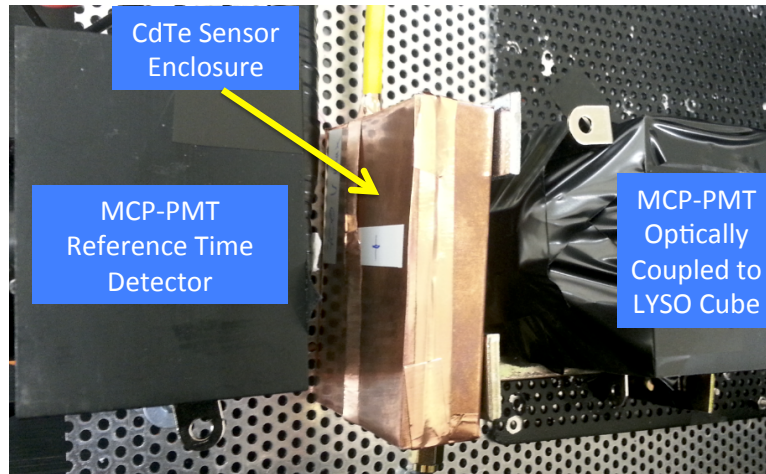


Figure 4: Photograph of the setup used in the T9 beam line. The reference timing MCP-PMT is located on the leftmost region of the photo, followed to the right by a scintillator counter, the copper box enclosing the CdTe sensor and an MCP-PMT optically coupled to a LYSO cube. The lead absorber is not present in the photo and was later inserted in front of the copper box.

measured by the wire chamber. Based on these plots, we can restrict our measurements to those electrons whose impact points are close to the center of the CdTe sensor.

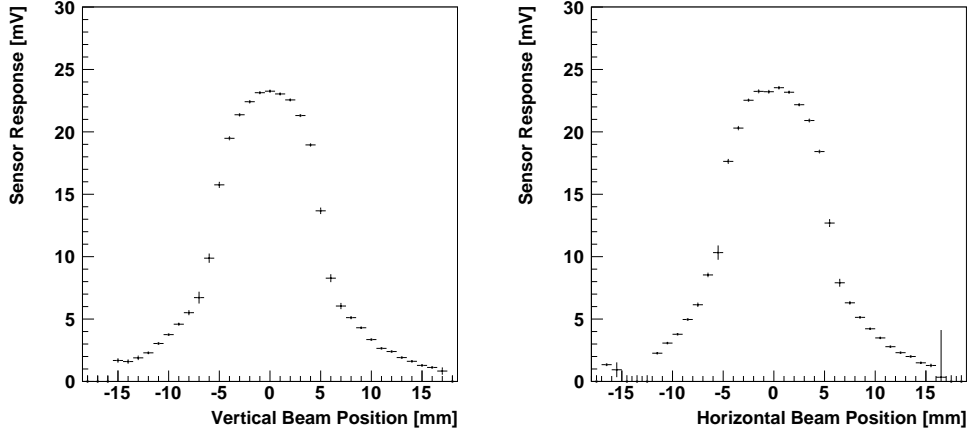


Figure 5: The average amplitude measured in the CdTe sensor is plotted as a function of the horizontal and vertical positions of the beam particle as measured by the wire chamber. The measurement shown was performed with electrons of 100 GeV and  $6 X_0$  of tungsten absorber.

#### 4. Event Reconstruction and Selection

All signals are recorded by the CAEN V1742 digitizer with a sampling time of 200 ps. The baseline pedestal for each channel is determined using the time samples outside of the signal window, and is subsequently subtracted from the signal pulses. An example of a recorded signal waveform in the CdTe sensor for an electromagnetic shower from a 100 GeV electron is shown in Figure 6. We did not observe an obvious energy dependency of the pulse shapes on the particle energy. The pulses feature two components, an initial faster one lasting about 15 ns followed by a component extending slightly beyond the 200 ns time window of our readout system. The drift velocity of electrons in CdTe is known to be much higher than for the holes [26], which may cause such a pulse shape. The relative size of the two signal components is observed to be independent of the energy of the incident electron, and therefore its energy may be determined from the fast component alone. Using randomly triggered data, we measured the RMS of the noise for the channel reading out the CdTe sensor after the amplifier to be about 1.3 mV.

The total charge collected in each channel is obtained by computing the integral of the pulse waveform over the full 200 ns range recorded by the digitizer. The time-stamp for each signal is reconstructed by fitting the pulse waveform with an appropriate functional form. For signal pulses from the MCP-PMTs, used as reference timers, we fit a Gaussian function to a 1.5 ns window around the peak of the pulse and extract the time-stamp  $t_0$  as the mean parameter of the Gaussian function. For signal pulses from the CdTe sensor, we fit a linear function to time sample points between 10% and 60% of the pulse maximum and the time-stamp  $t_1$  is assigned as the time at which the fitted linear function rises to

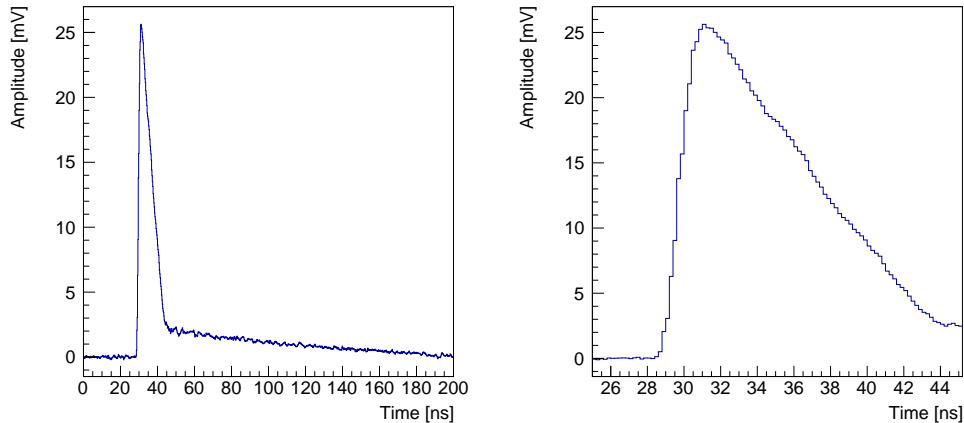


Figure 6: Examples of signal pulse in the CdTe sensor for electrons with energies of 100 GeV. The signal pulse shown was recorded by the CAEN V1742 digitizer after a 10 dB attenuator and a 36 dB fast amplifier. Right: Zoom in of the example pulse.

30% of the pulse maximum. More details of the time-stamp reconstruction can be found in reference [14].

For the measurements performed at the H2 beam-line, based on the results shown in Figure 5 we select events for which the incident beam particle lies within a region of size 3 mm by 3 mm about the center of the sensor. For the measurements performed at the T9 beam-line, the resolution of the wire chamber measurement was insufficient to make this requirement. We also require that the signal in the reference MCP-PMT detector has an amplitude larger than 25 mV. For data collected at the H2 beam-line, the MCP-PMT detector is located behind the absorbers and can discriminate between electrons that shower in the absorber material and pions that typically do not. We require that the signal amplitude in the MCP-PMT detector is larger than 500 mV to select a pure sample of electrons. For data collected at the T9 beam-line, the electron selection is performed using the LYSO scintillating crystal placed behind the absorber material and the CdTe sensor, as shown in Figure 3. The electromagnetic shower particles produce scintillation light in the LYSO crystal and are read out by an MCP-PMT. We require that the signal amplitude in the MCP-PMT coupled to the LYSO crystal is larger than 800 mV to select a sample of pure electrons. Furthermore, as the precision of the beam particle position measured by the wire chambers at the T9 beam-line is relatively poor, we also require large signals in the 1 cm  $\times$  1 cm scintillator trigger counter, with amplitude above 150 mV, to constrain the beam to a smaller geometric region.

## 5. Calorimetric Measurements

To obtain a preliminary characterization of the calorimetric performance of the CdTe sensors, we measure the total charge collected out of the CdTe sensor for various incident electron beam energies. Examples of the charge distributions are shown in Figure 7 for

177 2 GeV and 100 GeV electrons. For electrons with energy between 2 GeV and 7 GeV,  
 178 the sensor was placed after 2 radiation lengths of lead absorber, and for electrons with  
 179 energy above 50 GeV, the sensor was placed after approximately 6 radiation lengths of  
 180 three alternating layers of tungsten and lead.

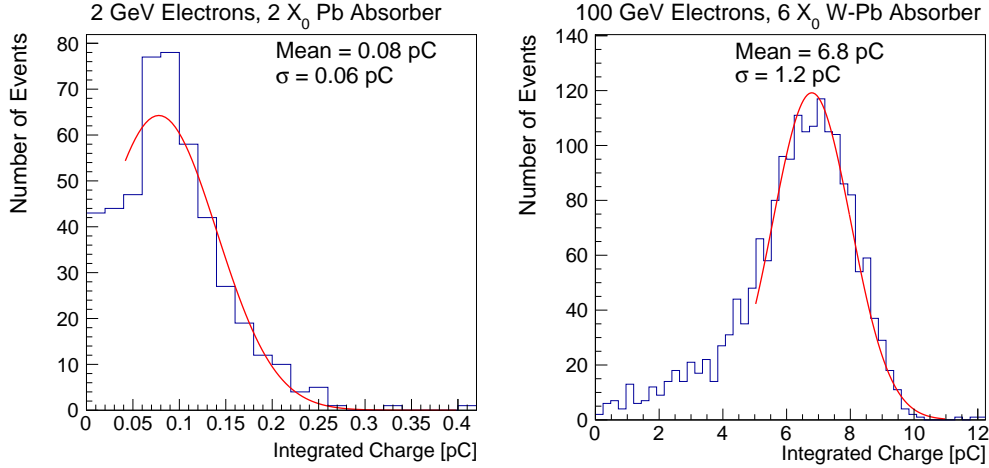


Figure 7: Distribution of total charge collected in the CdTe sensor for a 2 GeV electron after 2 X<sub>0</sub> of lead absorber (left) and a 100 GeV electron after 6 X<sub>0</sub> of tungsten and lead absorber (right). For the right plot, electrons are required to be within a 3 × 3 mm<sup>2</sup> area centered on the sensor. The accuracy of the wire chamber position measurement for the left plot was insufficient to make such a requirement.

181 We plot the mean collected charge as a function of the incident beam energy in  
 182 Figure 8 and observe that the signal size scales up with increasing beam energy. The  
 183 resolution is measured as the width parameter of a Gaussian fit to the charge distribution  
 184 and is shown by the green bars. The measured resolution ranges from about 80% for  
 185 electrons in the range of a few GeV to about 18% for electrons with an energy of 100 GeV.  
 186 The measurement at 100 GeV was made using events where the incident electron im-  
 187 pinged on a 3 × 3 mm area in the center of the sensor. This cut was not applied for the  
 188 data taken at the T9 beam-line as the position measurement resolution was insufficient.  
 189 These energy resolution measurements are encouraging given that they are performed  
 190 using only a single layer sample covering a relatively small transverse geometric area. In  
 191 future studies, we intend to improve the characterization of the calorimetric performance  
 192 by completing measurements of the longitudinal shower profile and to instrument a larger  
 193 transverse area to improve the transverse shower containment.

## 194 6. Timing Measurements

195 We characterize the timing performance of the CdTe sensor by measuring the time-  
 196 stamps relative to the MCP-PMT device used as a reference timer. An example of the  
 197 distribution of the time-stamp measurement for 100 GeV electrons after 6 X<sub>0</sub> of tungsten  
 198 absorber is shown in Figure 9. We extract the time measurement resolution from this  
 199 distribution as the width parameter of a Gaussian fit. In Figure 10 we show the measured



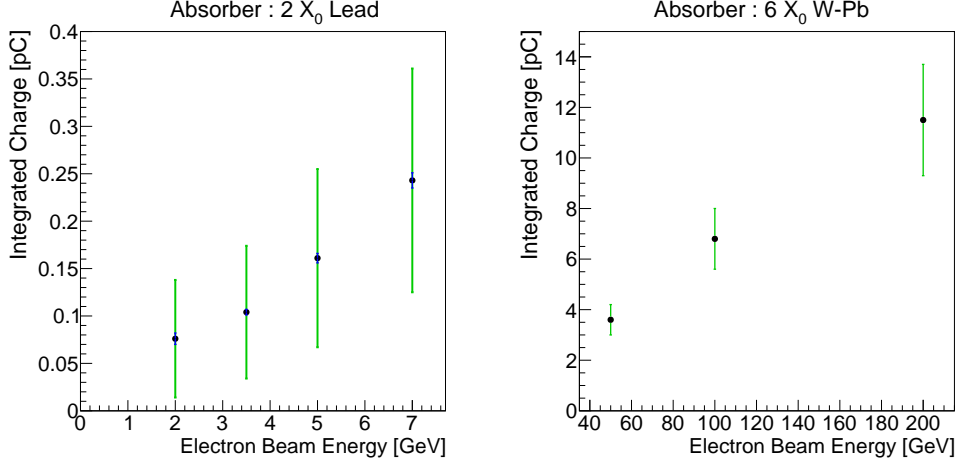


Figure 8: The mean charge collected in the CdTe sensor is plotted as a function of the electron beam energy. Left: Measurements performed at the T9 beam-line with 2  $X_0$  of lead absorber placed directly in front of the CeTe sensor. Right: Measurements performed at the H2 beam-line with 6  $X_0$  of tungsten absorber placed directly in front of the CeTe sensor. The blue bars show the uncertainty on the mean integrated charge extracted from the Gaussian fit to the charge distribution, while the green bars show the measured resolution.

time resolution as a function of the beam energy. For beam energies between 2 GeV and 50 GeV, the time resolution improves with increasing signal size as expected based on the increasing signal-to-noise ratio. However, above 100 GeV, the time resolution no longer improves with increasing signal size, which points towards some systematic limitation. We study a number of such factors in Section 6.1 below.

To further characterize the timing performance of the CdTe signals, we measure the rise-time, defined as the time for the signal to rise from 10% to 90% of its maximum amplitude, for various electron beam energies. The distribution of rise-time for 100 GeV electrons and the measured rise-time as a function of the beam energy are shown on the left and right of Figure 11 respectively. We observe a rise-time of around 1.3 ns that does not vary significantly with the beam energy.

### 6.1. Studies of Systematic Limitations on Time Resolution

One of the major systematic effects that have been observed in past timing studies [14–16] is the dependence of the time measurement on the amplitude of the signal. On the left of Figure 12, we show the dependence of the time-stamp measurement on the amplitude of the signal, and observe a mild dependence on amplitude, which we correct for in subsequent figures. On the right of Figure 12, we show the measured time resolution as a function of the signal amplitude and we observe a clear improvement in the resolution with increasing signal amplitudes up to 0.5 V. In this region, the impact of the signal-to-noise ratio is still the dominant factor for the time resolution.

We also study the dependence of the time-stamp measurement as a function of the geometric position of the incident beam particle as measured by the wire chambers in

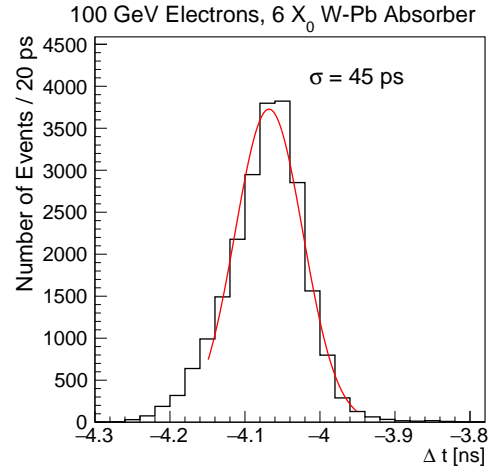


Figure 9: Distribution of the time-stamp measurement in the CdTe sensor for a 100 GeV electron after 6  $X_0$  of tungsten and lead absorber.

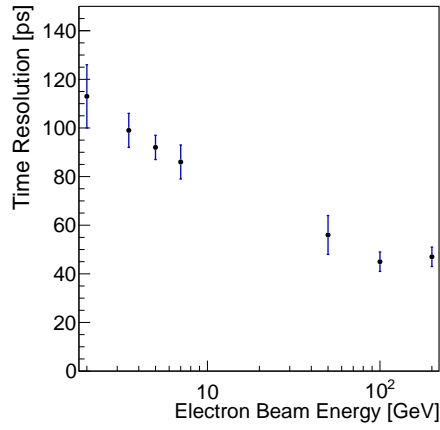


Figure 10: The measured time resolution of the CdTe sensor is plotted as a function of the electron beam energy.

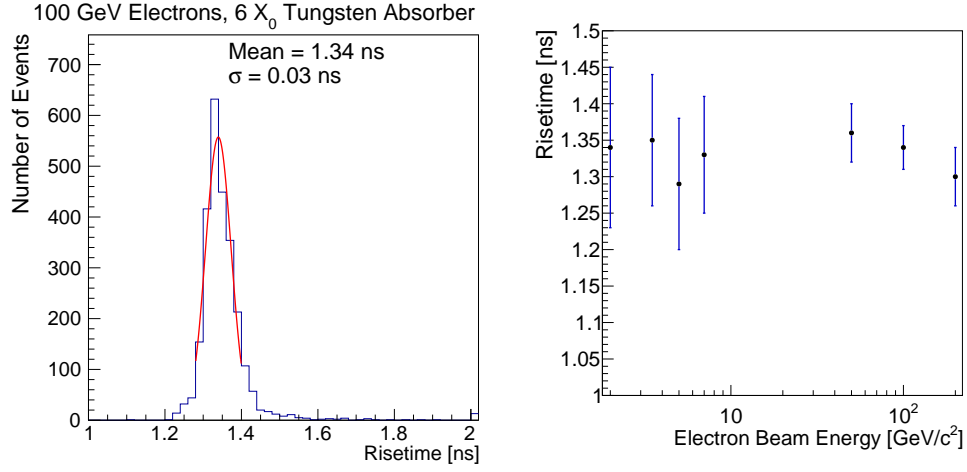


Figure 11: Left: Distribution of rise-time of the CdTe signal for 100 GeV electrons. Right: Rise-time of the CdTe signal is plotted as a function of the incident beam energy. The uncertainty is extracted from the width of the fitted gaussian to the rise-time distribution.

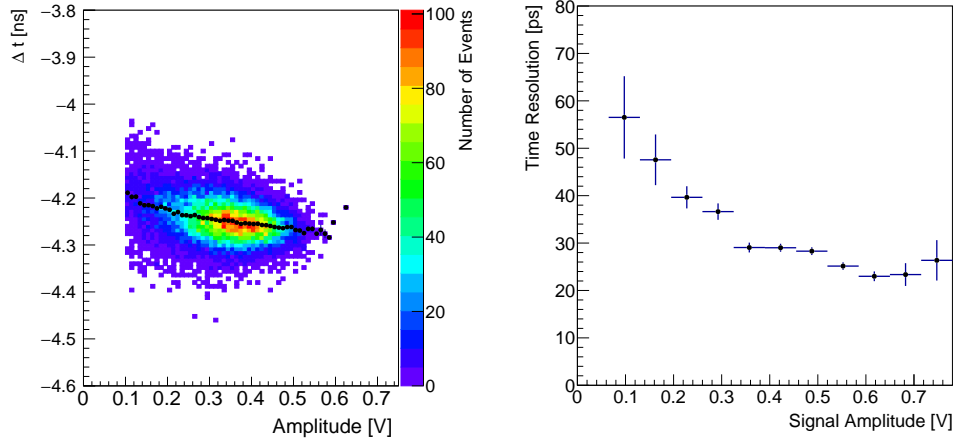


Figure 12: Left: The distribution of the signal amplitude in the CdTe sensor and the time measured in the CdTe sensor relative to the Photek reference detector is shown in the color scale. This data is from a 100 GeV electron beam after 6  $X_0$  absorber. The mean value of the time measured in the CdTe sensor as a function of the signal amplitude is shown in the black points. Right: The time resolution is measured as a function of the signal amplitude after correction for amplitude non-linearity.

Figure 13. A relatively large and linear dependence is observed, and this position non-uniformity of the time response adds significantly to the time resolution (about 37 ps). Performing a correction for this non-uniformity improves the time resolution from 45 ps to 25 ps for events with 100 GeV electrons. The distribution of time-stamps after correcting for the geometric position is shown in Figure 14. The measured time resolution, after correction for the position non-uniformity, has a mild dependence on the beam particle position and is shown in Figure 15. Combining the time resolution dependence on the horizontal and vertical beam positions, we measure the time resolution as a function of the planar distance between the beam position and the location of the back wire bond on the CdTe sensor, and observe a more clear dependence shown in Figure 16. More detailed studies are necessary to derive a better understanding of this effect. It will be crucial for any precision timing device using planar semi-conductor sensors to study the uniformity of the response to achieve an optimal performance.

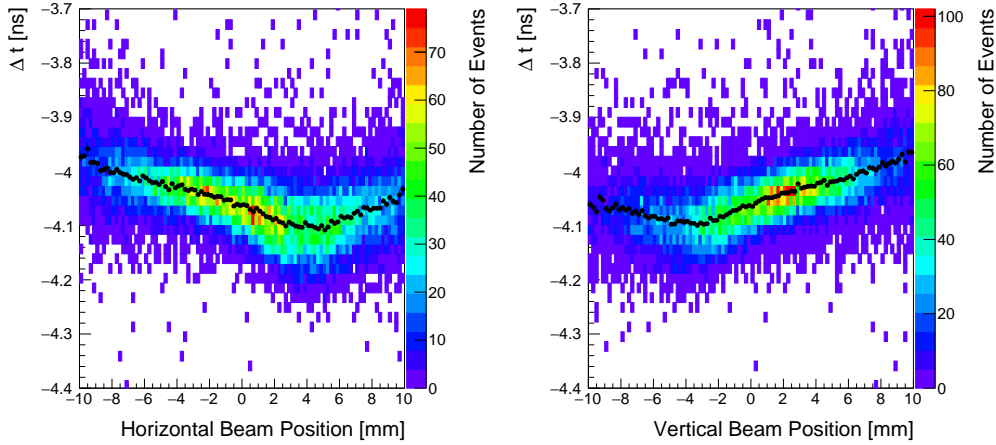


Figure 13: The distribution of the beam particle position measured by the wire chamber and the time measured in the CdTe sensor relative to the Photek reference detector is shown in the color scale. The mean value of the time measured in the CdTe sensor as a function of the beam particle position is shown in the black points. There is a dependence of the time difference on the impact point on the CdTe sensor which corresponds to about 100 ps across the CdTe sensor.

234

## 235 7. Discussion and Summary

236 In this article, we describe the first measurement of high energy electromagnetic  
 237 showers using CdTe sensors. These initial results are encouraging and motivate future  
 238 work on more detailed comparisons with simulation and more detailed measurements of  
 239 transverse and longitudinal shower profiles.

240 We have measured the rise time for signals in the Schottky type CdTe sensor diode to  
 241 be about 1.3 ns which makes them suitable as devices for precision timing applications.  
 242 The large ionization signal yield we achieve with a 1 mm thick sensor is equally favorable  
 243 for precision timing applications. We observe dependencies of the measured time on the

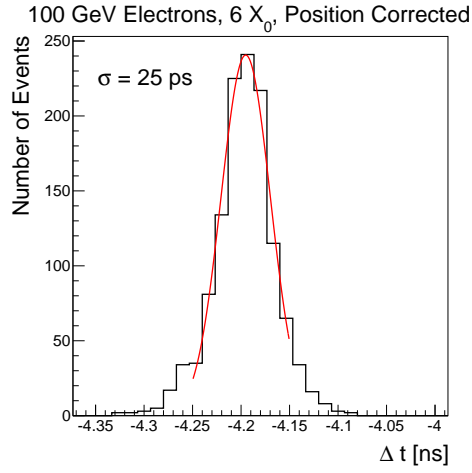


Figure 14: Distribution of the time-stamp measurement corrected for the geometric position non-uniformity in the CdTe sensor for a 100 GeV electron after 6  $X_0$  of tungsten absorber.

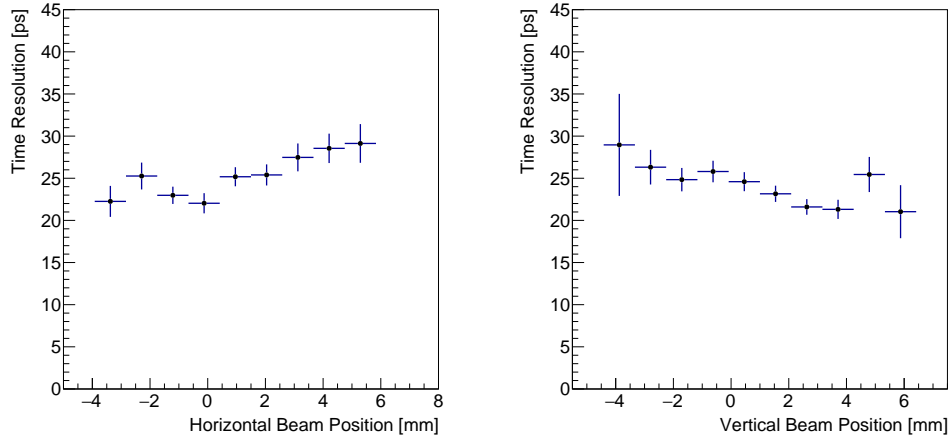


Figure 15: The time resolution is measured as a function of the horizontal (left) and vertical (right) beam position in a 2 mm wide region around the center of the sensor in the vertical (left) and horizontal (right) directions respectively.

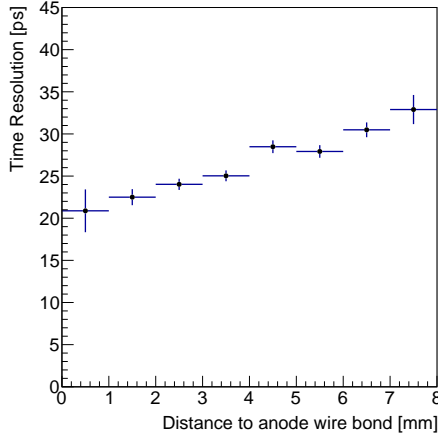


Figure 16: The time resolution is measured as a function of the planar distance of the incident beam particle to the back wire bond location on the sensor. The position non-uniformity of the time response as shown in Figure 13 has been corrected for. There remains a dependence of the measured resolution across the sensor, reaching 20 ps in the location closest to the back wire bond connection.

geometric position of the beam particle impact point on the sensor, which may indicate differences in the charge collection dynamics. More detailed studies of this aspect are needed and a more optimal design of the connection of the sensor readout is envisioned. Correcting for these dependencies yield time resolutions of 25 ps for a single layer CdTe sensor of transverse area  $1 \text{ cm} \times 1 \text{ cm}$ , uniformly sampled by the electromagnetic shower of electrons with energy above 100 GeV after 6 radiation lengths of tungsten and lead absorber. In the most favorable region of the sensor we observe time resolutions as low as 20 ps. These initial results are encouraging and motivate further in-depth studies in the future.

## 8. Acknowledgments

Supported by funding from California Institute of Technology High Energy Physics under Contract DE-SC0011925 with the United States Department of Energy. We thank the CERN test-beam facilities personnel for excellent beam conditions during our test-beam time. We also thank Paolo Meridiani and Francesco Micheli for their kind assistance on the setup of the DAQ system.

## References

- [1] A. Bornheim, “On the Usage of Precision Timing Detectors in High Rate and High Pileup Environments,” *PoS(Vertex2016)044*, 2016.
- [2] C. Adloff *et al.*, “Response of the CALICE Si-W electromagnetic calorimeter physics prototype to electrons,” *Nucl. Instrum. Meth. A*, vol. 608, pp. 372–383, 2009.
- [3] J. Butler, D. Contardo, M. Klute, J. Mans, and L. Silvestris, “Technical Proposal for the Phase-II Upgrade of the CMS Detector,” Tech. Rep. CERN-LHCC-2015-010. LHCC-P-008, CERN, Geneva, Jun 2015.

- [4] D. A. Jenny and R. H. Bube, "Semiconducting cadmium telluride," *Phys. Rev.*, vol. 96, pp. 1190–1191, Dec 1954.
- [5] P. Capper, *Properties of Narrow Gap Cadmium-Based Compounds*. INSPEC, 1994.
- [6] K. Zanio, "Purification of CdTe from, tellurium-rich solutions," *Journal of Electronic Materials*, vol. 3, no. 2, pp. 327–351, 1973.
- [7] A. R. Triboulet, Y. Marfaing and P. Siffert, "Undoped highresistivity cadmium telluride for nuclear radiation detectors," *Journal of Applied Physics*, vol. 45, no. 6, p. 2759, 1974.
- [8] F. V. Wald and G. Entine, "Crystal growth of CdTe for  $\gamma$ -ray detectors," *Nucl. Instrum. Meth. A*, vol. 150, no. 1, pp. 13 – 23, 1978.
- [9] A. Apresyan, G. Bolla, A. Bornheim, H. Kim, S. Los, C. Pena, E. Ramberg, A. Ronzhin, M. Spiropulu, and S. Xie, "Test beam studies of silicon timing for use in calorimetry," *Nucl. Instrum. Meth. A*, vol. 825, pp. 62 – 68, 2016.
- [10] H. F.-W. Sadrozinski, S. Ely, V. Fadeyev, Z. Galloway, J. Ngo, C. Parker, B. Petersen, A. Seiden, A. Zatserklyaniy, N. Cartiglia, F. Marchetto, M. Bruzzi, R. Mori, M. Scaringella, and A. Vinattieri, "Ultra-fast silicon detectors," *Nucl. Instrum. Meth. A*, vol. 730, pp. 226 – 231, 2013.
- [11] E. Rossa, C. Bovet, D. Meier, H. Schmickler, L. Verger, F. Mongellaz, and R. G., "CdTe Photoconductors for LHC Luminosity Monitoring," *CERN-SL-2000-068 BI*, 2000.
- [12] M. Filipenko, T. Gleixner, G. Anton, and T. Michel, "3D particle track reconstruction in a single layer cadmium-telluride hybrid active pixel detector," *Eur. Phys. J.*, vol. C74, no. 8, p. 3013, 2014.
- [13] E. Rossa, E. Gschwendtner, M. Placidi, H. Schmickler, A. Brambilla, F. Mongellaz, L. Verger, V. Cindro, M. Mikuz, and P. Moritz, "Fast Polycrystalline-CdTe Detector for LHC Luminosity Measurements," *CERN-SL-2002-001 BI*, 2002.
- [14] D. Anderson, A. Apresyan, A. Bornheim, J. Duarte, C. Pena, A. Ronzhin, M. Spiropulu, J. Trevor, and S. Xie, "On Timing Properties of LYSO-Based Calorimeters," *Nucl. Instrum. Meth. A*, vol. 794, pp. 7–14, 2015.
- [15] A. Ronzhin, S. Los, E. Ramberg, A. Apresyan, S. Xie, M. Spiropulu, and H. Kim, "Study of the timing performance of micro channel plate photomultiplier for use as an active layer in shower maximum detector," *Nucl. Instrum. Meth.*, vol. 795, pp. 288–292, 2015.
- [16] A. Ronzhin, S. Los, E. Ramberg, A. Apresyan, S. Xie, M. Spiropulu, and H. Kim, "Direct tests of micro channel plates as the active element of a new shower maximum detector," *Nucl. Instrum. Meth. A*, vol. 795, pp. 52 – 57, 2015.
- [17] A. Apresyan, S. Los, C. Pena, F. Presutti, A. Ronzhin, M. Spiropulu, and S. Xie, "Direct tests of a pixelated microchannel plate as the active element of a shower maximum detector," *Nucl. Instrum. Meth. A*, vol. 828, pp. 1 – 7, 2016.
- [18] D. Anderson, A. Apresyan, A. Bornheim, J. Duarte, C. Pena, A. Ronzhin, M. Spiropulu, J. Trevor, and S. Xie, "Precision Timing Calorimeter for High Energy Physics," *IEEE Trans. Nucl. Sci.*, vol. 63, no. 2, pp. 591–595, 2016.
- [19] D. Anderson *et al.*, "Precision Timing Measurements for High Energy Photons," *Nucl. Instrum. Meth.*, vol. A787, pp. 94–97, 2015.
- [20] J. Beringer *et al.*, "Review of Particle Physics (RPP)," *Phys. Rev.*, vol. D86, p. 010001, 2012.
- [21] "AcroRad Co., Ltd.," <http://www.acrorad.co.jp/>.
- [22] S. Ritt, R. Dinapoli, and U. Hartmann, "Application of the DRS chip for fast waveform digitizing," *NIM A* 623 (2010) 486–488.
- [23] [http://http://www.hamamatsu.com/resources/pdf/etd/C5594\\_TACC1068E.pdf](http://http://www.hamamatsu.com/resources/pdf/etd/C5594_TACC1068E.pdf).
- [24] [http://www.hamamatsu.com/resources/pdf/etd/R3809U-50\\_TPMH1067E09.pdf](http://www.hamamatsu.com/resources/pdf/etd/R3809U-50_TPMH1067E09.pdf).
- [25] [http://www.photek.com/pdf/datasheets/detectors/DS006\\_Photomultipliers.pdf](http://www.photek.com/pdf/datasheets/detectors/DS006_Photomultipliers.pdf).
- [26] J. Fink, P. Lodomez, H. Kruer, H. Pernegger, P. Weilhammer, and N. Wermes, "TCT characterization of different semiconductor materials for particle detection," *Nucl. Instrum. Meth. A*, vol. 565, no. 1, pp. 227 – 233, 2006.